Design, fabrication and testing of a micromachined thermo-optical light modulator based on a vanadium dioxide array

2004 J. Micromech. Microeng. 14 833

(http://iopscience.iop.org/0960-1317/14/7/001)

INSTITUTE OF PHYSICS PUBLISHING JOURNAL OF MICROMECHANICS AND MICROENGINEERING

J. Micromech. Microeng. **14** (2004) 833–840 PII: S0960-1317(04)71758-1

Design, fabrication and testing of a micromachined thermo-optical light modulator based on a vanadium dioxide array

Lijun Jiang and William N Carr

New Jersey Institute of Technology, University Heights, Newark, NJ 07102, USA

E-mail: carr@adm.njit.edu

Received 11 November 2003, in final form 16 February 2004
Published 13 May 2004
Online at stacks.iop.org/JMM/14/833
DOI: 10.1088/0960-1317/14/7/001

Abstract

In this paper, a thermal-optical light modulator was developed based on a surface micromachined vanadium dioxide (VO_2) array. VO_2 thin film undergoes a reversible semiconductor-to-metal phase transition at about 68 °C, which is accompanied by an abrupt transformation from a transparent semiconductor phase at low temperature to a reflective metallic state at high temperature. To exploit this phase-transition related thermo-optical switching, low-thermal-mass pixels with long and thin supporting legs were surface micromachined above a glass substrate to achieve good thermal isolation between pixels and ensure fast enough switching speed. The pixel design was optimized by thermal and optical simulations. Active VO_2 thin film was fabricated by e-beam evaporation of vanadium metal film followed by oxidation. The deposited VO_2 film exhibits a grain structure and undergoes a phase transition at 65 °C with about 15 °C hysteresis. A surface micromachining process was developed to realize a light modulator with 64 × 64 pixels. The light switching and modulation ability of the VO_2 array was experimentally tested and demonstrated. Further study shows that the surface micromachining process has no degrading effect on the optical property of VO_2 film.

1. Introduction

Micromachined devices are well suited for photonic modulations, with their miniaturized dimensions and mirror-smooth surfaces [1]. Today a wide variety of micromachined light modulators have been developed based on the effects of reflection, transmission, interference or diffraction. Most micromachined light modulators rely on certain mechanical actuation mechanisms, which add challenges in terms of fabrication complexity and reliability. In this paper, we present a thermo-optical light modulator array, with active VO_2 thin films, that is not mechanically actuated. The modulation of the light is controlled by the pixel temperature. This is the first time that a VO_2 light modulator has been realized by surface micromachining.

At room temperature, vanadium dioxide is a semiconductor with monoclinic crystal symmetry and transforms to a metallic phase with a tetragonal structure at about 68 °C [2]. The semiconductor-to-metal phase transition is accompanied by drastic changes in its electrical and optical properties. As large as four or five orders of electrical resistivity variation has been observed for VO_2 single crystal or oriented polycrystalline films [3]. Optically, VO_2 film is transparent in the semiconductor phase and highly reflective in the metallic state. The phase-transition temperature is conveniently close to room temperature and can be further reduced by doping [4]. All above properties make VO_2 a

good candidate material for optical sensing and switching applications [5]. Several light modulators have been proposed based on the thermal-optical switching property of bulk VO_2 thin films [6–8]. However, there are several disadvantages in using bulk VO_2 film for spatial light modulators. First, the thermal cross talk is severe between adjacent pixels. Second, the switching speed is slow due to the large thermal mass of bulk film. To increase the cooling speed, it has been suggested that micro-fluidic channels be integrated under each pixel [9], which itself has the disadvantages of high fabrication complexity and low fill factor. In this paper, we use surface micromachining technology to fabricate a large format, high uniformity and high speed VO_2 modulator based on pixel array structures. First, because the optical property of VO_2 is extremely temperature-sensitive, good thermal isolation is required to prevent cross talk between adjacent pixels and temperature deviations across the array. Second, the thermal mass of the pixel needs to be minimized to compensate for the high thermal isolation for fast enough switching speed. The above requirements are accommodated with surface micromachining technology.

A 64 × 64 VO_2 light modulator has been fabricated by surface micromachining. The VO_2 pixel design was optimized by thermal and optical simulations. Active VO_2 thin film was fabricated by evaporation of vanadium film followed by thermal oxidation and integrated into the microfabrication by lift-off. In this paper, the results of the design, fabrication and testing of the VO_2 light modulator will be presented.

2. Design and analysis

2.1. Structure and principle

A schematic drawing of an individual VO_2 light modulator pixel is shown in figure 1. The membrane pixel is micromachined from low thermal conductive silicon dioxide (SiO_2) thin film. The long, thin supporting legs provide good thermal isolation between adjacent pixels. Vanadium dioxide film is deposited on the top of the SiO_2 membrane. The modulation of the light is achieved based on the variation of the optical reflectance or transmittance of the VO_2 film at its phase transition. The general operation principle of the light modulator is as follows: at the idle state, the array is stabilized at its low-temperature semiconductor state. Momentary heat injection into the VO_2 pixel will drive it into the high-temperature metallic state. An optical contrast is produced between pixels with different temperatures. The temperature can be controlled using an integrated resistive heater on each pixel or spatially addressed thermal radiation sources. The temperature differentials between adjacent pixels will produce sharp optical contrasts. Initial design is an array with 64 × 64 pixels. The optimum structural design of the VO_2 modulator pixel is achieved by considering both its thermal and optical properties, which will be discussed in next two sections.

2.2. Thermal analysis

In the aspect of thermal design, the primary goal is to achieve good thermal isolation between pixels to prevent thermal cross

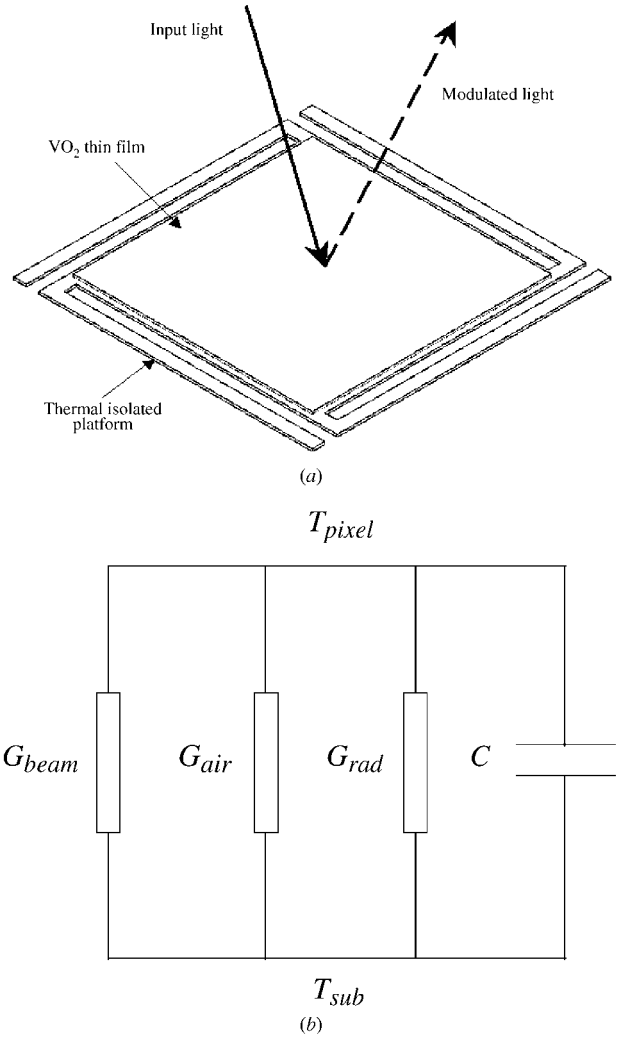

Figure 1. (*a*) Schematic drawing and (*b*) thermal lumped circuit model of an individual VO_2 pixel.

talk. For a microstructure as shown in figure 1, the equation that governs the heat flow is

$$C\frac{\mathrm{d}(\Delta T)}{\mathrm{d}t} + G(\Delta T) = P \tag{1}$$

where C and G are the heat capacity and thermal conductance of the pixel, respectively; P is the momentary thermal power that enters or leaves the pixel. The lumped thermal circuit model of the pixel is shown in figure 1(*b*). The thermal time constant of the pixel is derived by analogy to the RC time constant and is given by

$$\tau = \frac{C}{G}. \tag{2}$$

The thermal mass is the summation of the heat capacity of all the layers in the pixel and calculated as

$$C = V\rho c \tag{3}$$

where V is the volume, ρ is the density, and c is the specific heat of the material.

The thermal conductance consists of three independent parts, including the heat conductance through the supporting beams (G_{beams}), the conductance by the ambient (G_{air}), and

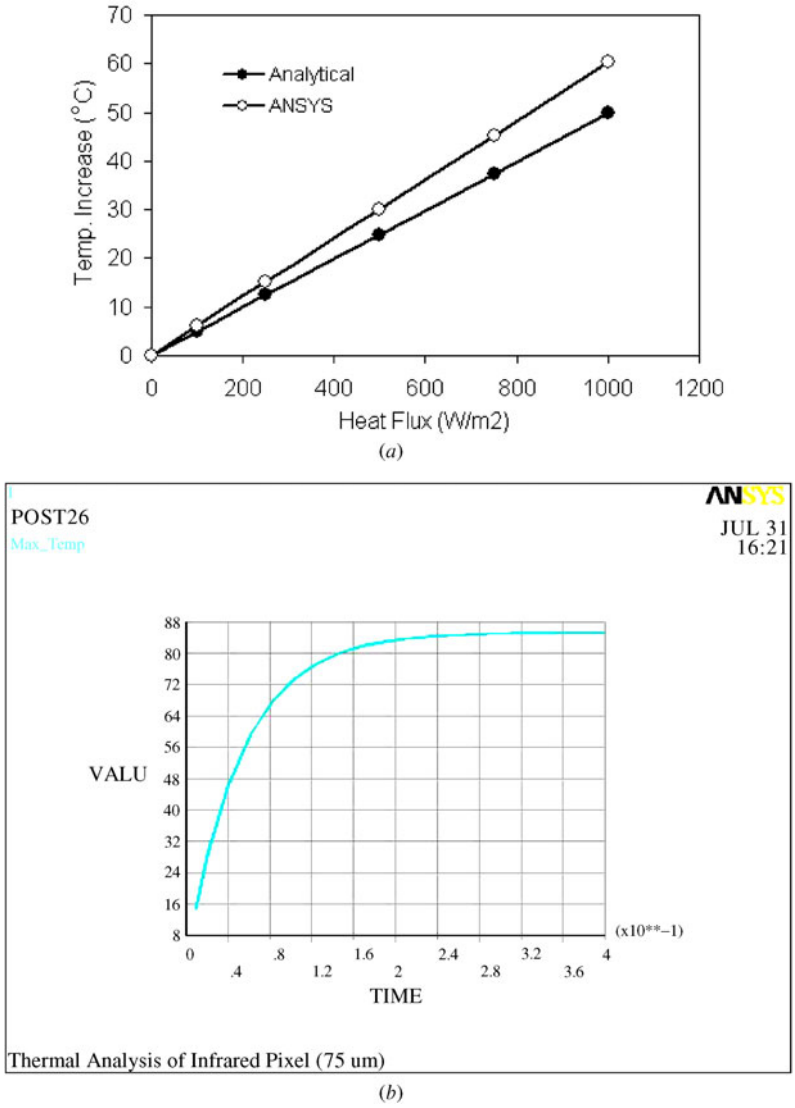

Figure 2. Finite element simulation results of (*a*) pixel temperature increase under different heat inputs and (*b*) transient thermal response.

the radiation from the pixel surface (G_{rad}). The total thermal conductance is the summation of the three components:

$$G = G_{\text{beams}} + G_{\text{air}} + G_{\text{rad}}. \tag{4}$$

The radiation conductance is the ultimate low limit for the thermal isolation pixel and can be expressed as

$$G_{\text{rad}} = 4\sigma\varepsilon_{\text{e}}A_{\text{pixel}}T^3 \tag{5}$$

where σ is the Stefan–Boltzmann constant, ε_{e} is the effective emissivity, A_{pixel} is the area of both the front and bottom pixel surface, and T is the absolute temperature of the pixel.

The conductance by the ambient consists of both conduction and convection. The pixel will operate in a vacuum and the convective effect is minimal. The ambient heat conduction is expressed as

$$G_{\text{air}} = \lambda_{\text{air}}\frac{A_{\text{pixel}}}{d} \tag{6}$$

where the λ_{air} is the thermal conductivity of the air and d is the space between the pixel and substrate.

The thermal conductance by the beams is determined by the pixel dimension and the thermal conductivity of the beam material, which can be calculated as

$$G_{\text{beam}} = 4\lambda_{\text{SiO2}}\frac{A_{\text{beam}}}{L_{\text{beam}}} \tag{7}$$

where λ_{SiO2} is the thermal conductivity of the SiO_2 beam material, A_{beam} and L_{beam} are the area and length of the beam respectively. The number 4 is the number of beams for each pixel. In our work and from [10], it has been shown that in most situations the thermal conductance by the beams dominates and the conductance by the air conduction and surface radiation can be neglected.

The thermal mass and conductance of the pixel were calculated and the thermal time constant was derived from them. A 3D (three-dimensional) finite element solid model was set up in ANSYS 6.1. A thermal brick element with 8 nodes was used. The fixed ends of the beams are set to constant room temperature. A steady-state simulation gives the balanced temperature distribution of the pixel. Figure 2(*a*) shows the temperature increase of the pixel under different heat

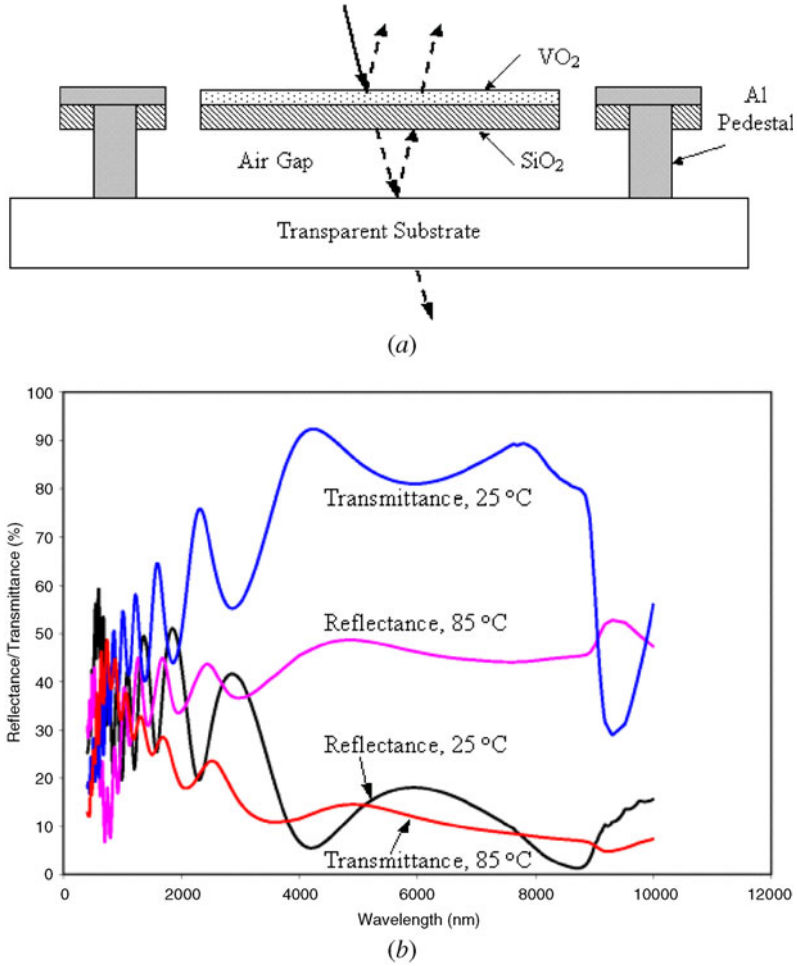

Figure 3. (*a*) Cross section view of the pixel structure used in the optical simulation. (*b*) Simulated transmittance and reflectance spectra of the VO_2 pixel.

power inputs. The small disagreement between the analytical calculation and simulation results is because only the thermal resistivity of the beam was considered in the calculation. The thermal time constant was derived from a transient thermal simulation, as shown in figure 2(*b*). The thermal time constant (∼50 ms) is relatively large in this design but is expected to decrease one or two orders when a heating resistor is integrated onto each pixel, which will increase the thermal conductance of the beam significantly.

2.3. Optical model

The VO_2 light modulator pixel structure consists of several layers of thin films, whose optical characteristics can be calculated based on multilayer matrix formulation [11]. For an assembly with q layers, the transmittance T_q and reflectance R_q are given by

$$T_q = \frac{4\eta_0 \,\mathrm{Re}\,(\eta_s)}{(\eta_0 B + C)\,(\eta_0 B + C)^*}$$
$$R_q = \left(\frac{\eta_0 B - C}{\eta_0 B + C}\right)\left(\frac{\eta_0 B - C}{\eta_0 B + C}\right)^* \qquad (8)$$

in which B and C are the normalized electric and magnetic fields at the front interface, and are calculated from the characteristic matrix,

$$\begin{bmatrix} B \\ C \end{bmatrix} = \left\{ \prod_{m=1}^{q} \begin{bmatrix} \cos\delta_m & \mathrm{i}\sin\delta_m/\eta_m \\ \mathrm{i}\eta_m \sin\delta_m & \cos\delta_m \end{bmatrix} \right\} \begin{bmatrix} 1 \\ \eta_s \end{bmatrix} \qquad (9)$$

where m denotes the mth layer of film, s denotes substrate or exit medium. The other symbols are $\delta_m = 2\pi N_m d_m \cos\theta_m/\lambda$ and the tilted optical admittance $\eta_m = H_m/E_m$ that relates the electric field E_m and magnetic field H_m.

In this research, the effect of the changing refractive index of VO_2 thin film combined with the underlying layers defined the optical properties of the light modulator. It was calculated based on the matrix formulation using commercial thin film optics software of Essential-Macleod^{TM} [12]. The simulated structure consists of a glass substrate, a 2.25 μm air gap, 200 nm silicon dioxide and 50 nm vanadium dioxide (figure 3(*a*)). The VO_2 refractive index data before and after its phase transition were obtained from [13]. Figure 3(*b*) shows the simulated transmittance and reflectance spectra of the VO_2 pixel before and after the phase transition. Periodic interference characteristics were observed in the visible region and the optical contrast enlarged with the increasing of wavelength into infrared region.

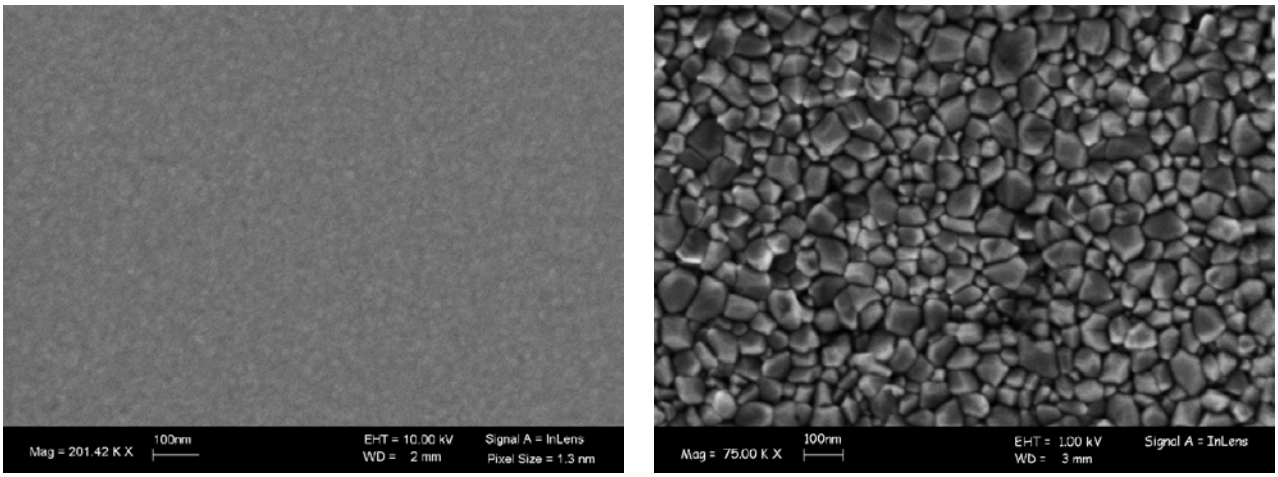

(*a*) (*b*)

Figure 4. Surface structure micrograph of (*a*) as-deposited vanadium film and (*b*) thermally oxidized VO_2 thin film.

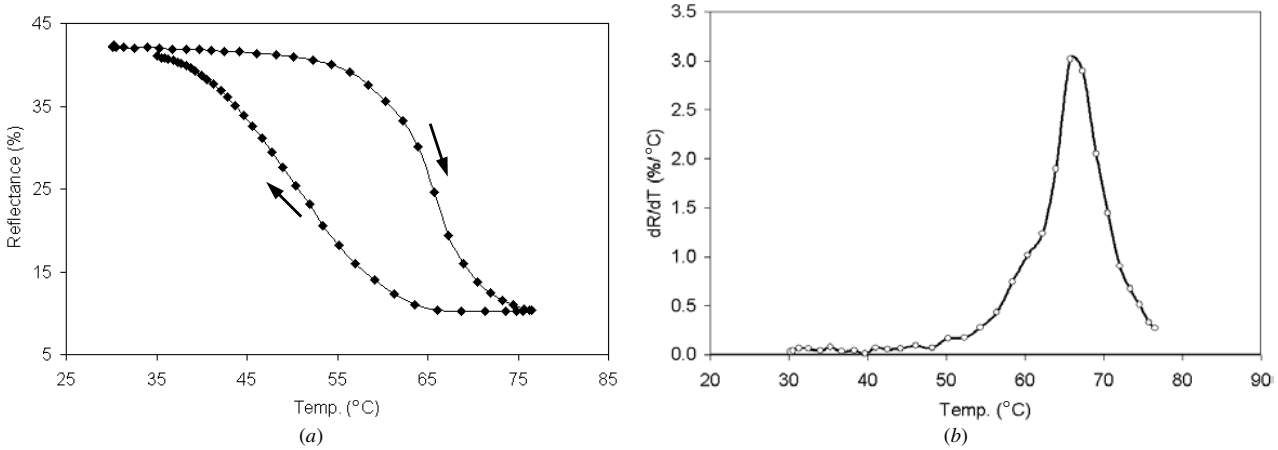

(*a*) (*b*)

Figure 5. (*a*) Measured temperature–reflectance curve and (*b*) its phase transition temperature of thermally oxidized VO_2 film.

3. Experimental results

3.1. Synthesis of VO_2 thin film

A wide range of deposition methods have been reported to deposit VO_2 thin films, including reactive sputtering [14], reactive evaporation [15], chemical vapor deposition [16], pulsed laser ablation [17], as well as sol-gel methods [18]. In this study, VO_2 thin film was fabricated by e-beam evaporation of vanadium metal followed by thermal oxidation into vanadium oxide in room ambient. The oxidation process has been optimized in terms of thermo-optical modulation and was described in detail elsewhere [19]. As-deposited vanadium film shows a smooth surface with no observable features at 200 000 times magnification under a scanning electron microscope. After oxidation, the VO_2 thin film exhibits a surface microstructure of a columnar grain structure with average grain size of less than 100 nm (figure 4).

The thermo-optical switching property of the deposited VO_2 film was tested with a laser-photodiode set-up. The VO_2 thin film was mounted on a temperature-controlled heater stage. A 635.5 nm red laser was used as the optical source, which was chopped at 10 kHz. The reflected laser beam by the VO_2 film is detected with a reverse-biased photodiode. The output of the photodiode was picked up with a lock-in amplifier, which suppresses the noise of the stray light. Figure 5 shows the measured hysteretic temperature–reflectance curve of one of the VO_2 samples. There is a hysteresis of about 15 °C between the heat-up branch and cool-down branch. The hysteresis width is larger than the crystalline oriented film [3]. It can be explained by the grain microstructure as we have seen in figure 4. The surface microstructure of the oxidized VO_2 film consists of a host of grains. Each grain has its own phase-transition temperature and undergoes phase transition independently, which results in a broadened hysteresis. If we define the phase-transition temperature (T_c) as the point where the temperature–reflectance curve shows the sharpest slope at the heat-up branch, we get a T_c of about 65 °C. It is comparable to the data of the VO_2 films deposited by other methods [14–18].

3.2. Microfabrication and characterization results

A surface micromachining process has been developed to fabricate the VO_2 light modulator. A polyimide sacrificial layer was used. The VO_2 thin film was patterned by vanadium metal lift-off followed by oxidation. The microfabrication

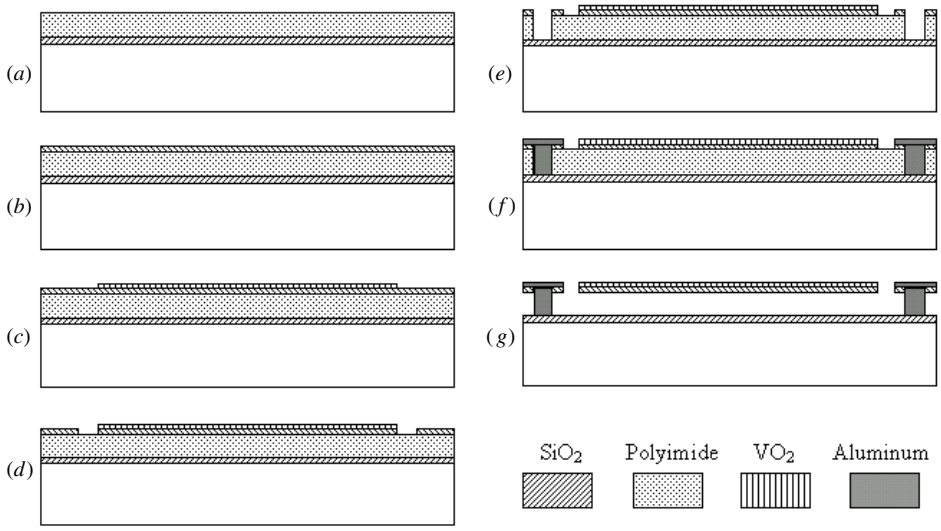

Figure 6. Main fabrication process.

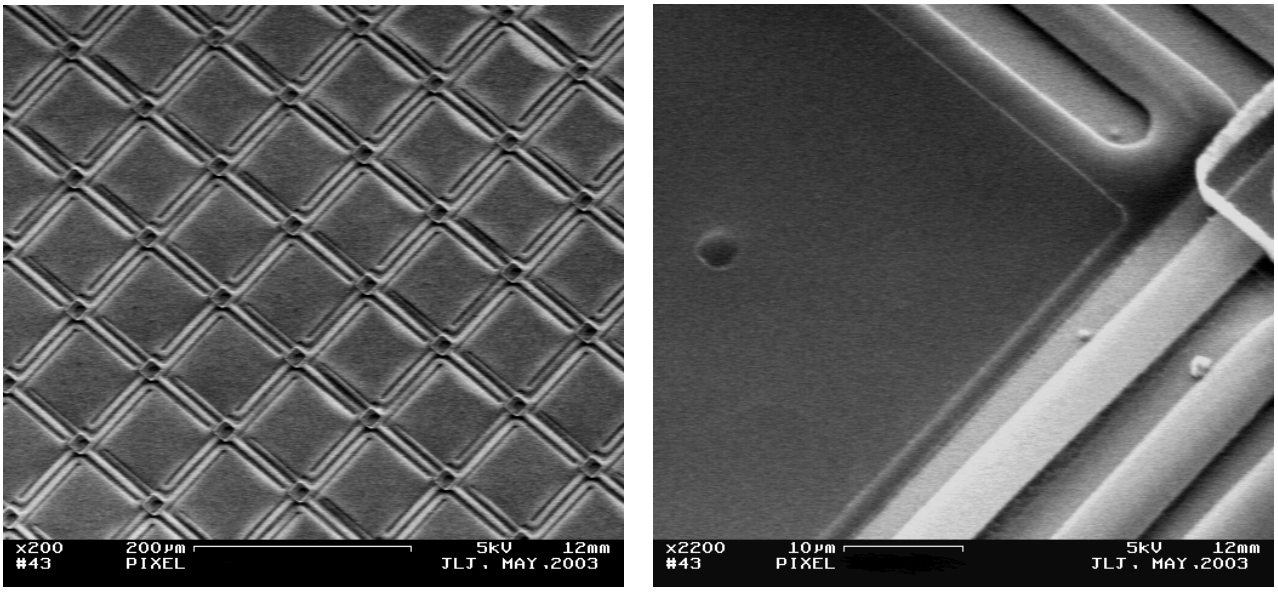

(*a*) (*b*)

Figure 7. Micrograph of selected area of the fabricated VO_2 array (*a*) with a close-up view (*b*).

process is briefly illustrated in figure 6. The starting substrate was a 4 inch glass wafer. First, a sacrificial layer of polyimide is spun on the substrate and cured at 400 °C. A final thickness of 2.25 μm was achieved by adjusting the spin and spreading speed (*a*). Next, 200 nm SiO_2 thin membrane is deposited on top of polyimide by plasma-enhanced chemical vapor deposition (PECVD) at 240 °C with silane and methane precursors (*b*). The active VO_2 film is integrated by vanadium metal lift-off followed by thermal oxidation. The target thickness of the VO_2 film was 50 nm (*c*). Then the SiO_2 is patterned into the thermal isolation pixels with CHF_3 reactive ion etching (*d*). Next, the SiO_2 and polyimide were etched with CF_4 + O_2 plasma etching for the pedestal opening (*e*). The pedestal is formed by aluminum metal which was patterned by lift-off (*f*). Finally, after dicing and separation into individual chips, the structure is sacrificially released in an ambient-pressure oxygen plasma barrel etcher (*g*).

Figure 7 shows the micrographs of the selected pixels of the fabricated VO_2 light modulator array, with a close-up view of the VO_2 thin films on single pixel. After microfabrication, the transmittance spectra before and after the phase transition were taken on a VO_2 thin film testing structure, which is directly on the glass substrate and not released. Figure 8 shows the measurement result. An optical contrast of ∼90% to ∼30% was observed in the near-infrared region. A good agreement between the measurement and simulation results was noted.

The switching behavior of the pixel array was characterized with a LED–CCD set-up. The light modulator chip with fully released pixels was mounted on a thermoelectric device. A ring of light emitting diodes (LED, peak wavelength = 630 nm) was used as a light source. The light of the LED was reflected by the VO_2 array and detected with a CCD camera. The temperature of the VO_2 array was

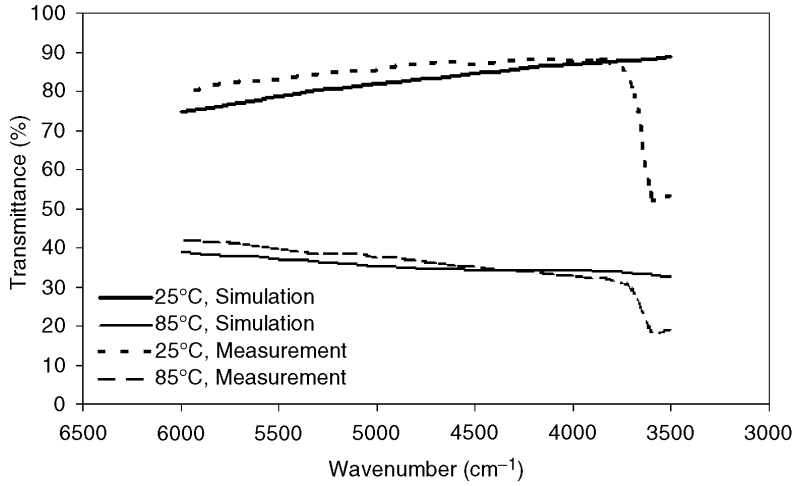

Figure 8. Comparison of the measured and simulated transmittance spectra of the VO_2 film test structure.

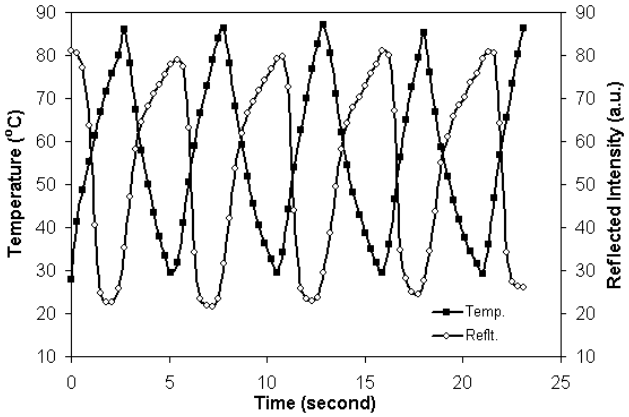

Figure 9. Measured reflectance variation and change of pixel temperature of the VO_2 light modulator array.

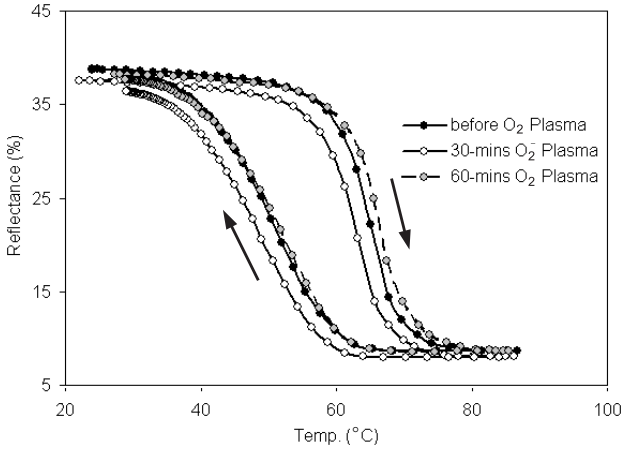

Figure 10. Measured temperature–reflectance curves for VO_2 films after different times of O_2 plasma treatment.

switched between 30 °C and 90 °C by the thermoelectric device. The light was modulated by the temperature-controlled reflectance of the VO_2 pixels. The CCD camera was focused on the pixel array surface. Both the temperature and the light intensity variations were recorded synchronously with a computer. Figure 9 shows the measured intensity variation of the reflected light with the VO_2 temperature. The relatively low switching speed was limited by the large thermal time constant of the thermoelectric device. The thermal constant of the VO_2 pixel needs to be measured in further experiments. In figure 9, a reversed visible switching behavior is observed compared to the result in the infrared range (figure 8). It is because the combination of the refractive index and film thickness at high temperature is close to anti-reflection conditions for the visible wavelength in the test. Consequently, the high-temperature metallic state actually shows lower reflectance than the low-temperature semiconductor state in this special case.

3.3. Effect of O_2 plasma

There are potential concerns that the microfabrication processes may change the optical property of the VO_2 thin film. The processing steps after the VO_2 deposition include photolithography, reactive ion etching, and O_2 plasma sacrificial releasing. In the photolithography and reactive ion etching steps, the VO_2 thin film was covered by photoresist, which was not likely to affect its properties. The only step that may modify VO_2 properties is the final releasing in O_2 plasma, in which the VO_2 film is exposed directly to the high-temperature (∼240 °C) reactive plasma. To test the effect of the O_2 plasma on the VO_2 film, testing films were put in O_2 plasma for different durations and their reflectance switching was measured and compared. Figure 10 shows the measurement result. There is no obvious change observed in terms of the optical contrast magnitude before and after the phase transition. The shift of the phase-transition temperature as shown is believed to be from the experimental measurement instead of actual effect.

4. Conclusions

In this paper, the well-known thermo-optical switching of VO_2 thin film was utilized to create a miniaturized light modulation device. To prevent thermal cross talking, thermal isolated pixels were surface micromachined above the substrate. The

thermal property was simulated with ANSYS 6.1, which predicted a thermal conductance of 10^{-7} W K^{-1} and time constant less than 50 ms. Optical design was based on multilayer matrix formulation that takes into consideration the temperature-dependent refractive index of VO_2. A deposition process for VO_2 thin film has been developed using e-beam evaporation of vanadium metal followed by thermal oxidation. A light modulator array with 64 $\times$ 64 pixels was fabricated by surface micromachining with polyimide as a sacrificial layer. A metal lift-off step was used to pattern the VO_2 film. The final release was done in oxygen plasma. Experimental testing was done on both test structures and fully released VO_2 arrays. The light modulation behavior was demonstrated by a reflection switching (4 to 1 ratio) of visible LED light. Spectral measurement reveals a 90% to 30% modulation contrast in the near-infrared region. The effect of the oxygen plasma on VO_2 film was investigated. No degrading change in its optical switching was observed for a VO_2 film that underwent 1 h O_2 plasma treatment.

In future work, the optical properties in the infrared region need to be characterized. For the visible wavelength, the optical contrast between low-temperature and high-temperature states needs to be enhanced by improved optical thin film structure design.

References

[1] Senturia S D 2001 *Microsystem Design* (Dordrecht: Kluwer)

[2] Morin F J 1959 Oxides which show metal-to-insulator transition at the Neel temperature *Phys. Rev. Lett.* **3** 34–6

[3] De Natale J F, Hood P J and Harker A B 1989 Formation and characterization of grain-oriented VO_2 thin films *J. Appl. Phys.* **66** 5844–50

[4] Burkhardt W, Christmann T, Franke S, Kriegseis W, Meister D, Meyer B K, Niessner W, Schalch D and Scharmann A 2002 Tungsten and fluorine co-doping of VO_2 films *Thin Solid Films* **402** 226–31

[5] Jerominek H, Picard F and Vincent D 1993 Vanadium oxide films for optical switching and detection *Opt. Eng.* **32** 2092

[6] Coath J A and Richardson M A 1998 An infrared reflective optical modulator *Proc. SPIE* **3292** 116–20

[7] Richardson M A and Coath J A 1998 Infrared optical modulators for missile testing *J. Opt. Laser Tech.* **30** 137–40

[8] Billingsley J D 1985 Dynamic Infrared Scene Projector *US Patent Specification* 4530010

[9] Blodgett D W, Lange C H and McNally P J 1993 Vanadium-dioxide-based infrared spatial light modulators *Proc. SPIE* **1969** 349–56

[10] Eriksson P, Andersson J Y and Stemme G 1997 Thermal characterization of surface-micromachined silicon nitride membranes for thermal infrared detectors *IEEE J. MEMS* **6** 55–61

[11] Macleod H A 2001 *Thin-Film Optical Filters* (Bristol: Institute of Physics Publishing)

[12] Thin Film Center Inc., 2745 E Via Rotonda, Tucson, AZ 85716, USA

[13] Verleur H W, Barker A S and Berglund C N 1968 Optical properties of VO_2 between 0.25 and 5 eV *Phys. Rev.* **172** 788–98

[14] Chain E E 1987 Effects of oxygen in ion-beam sputter deposition of vanadium oxide *J. Vac. Sci. Technol.* A **5** 1836–9

[15] Nyberg G A and Buhrman R A 1987 High optical contrast in VO_2 films due to improved stoichiometry *Thin Solid Films* **147** 111–6

[16] Maruyama T and Ikuta Y 1993 Vanadium dioxide thin films prepared by chemical vapor deposition from vanadium (III) acetylacetonate *J. Mat. Sci.* **28** 5073–8

[17] Kim H K, You H, Chiarello R P, Chang H L M, Zhang T J and Lam D J 1993 Finite-size effect on the first-order metal-insulator transition in VO_2 films grown by metal-organic chemical-vapor deposition *Phys. Rev.* B **47** 12900–7

[18] Yin D, Xu N, Zhang J and Zheng X 1996 Vanadium dioxide films with good electrical switching property *J. Phys. D: Appl. Phys.* **29** 1051–7

[19] Jiang L and Carr W N 2003 Vanadium dioxide thin films for thermo-optical switching presented *2003 MRS Fall Meeting (Boston)*